The calculated errors for the various measurements show them to be generally satisfactory - with one exception, that for the orifice flowmeter at flowrates of 30 l/s and below. However, at these flowrates the vortex flowmeter has a satisfactory accuracy, and was not susceptible to cavitation at those flowrates.

The calculated values also are shown to have generally satisfactory errors, the exceptions being for the cavitation indices (σ_1 and σ_2) for upstream pressures of 2000 kPa and 3000 kPa, the errors for 2000 kPa being greater than for 3000 kPa, this holds true also for the 0,206 d/D orifice rather than for the other orifice sizes. This is as a result of the error increasing as the pressure decreases. The effect of this on experimental results is discussed later.

5.2.3 DISCUSSION OF RESULTS

To aid the interpretation and discussion of experimental incipient cavitation results the following graphs were drawn (for constant upstream pressure):

UPSTREAM PRESSURE	vs	PRESSURE DROP	FIGURE 5.12
UPSTREAM PRESSURE	vs	PIPE FLOW VELOCITY	FIGURE 5.13
UPSTREAM PRESSURE	vs	REYNOLDS NUMBER	FIGURE 5.14
UPSTREAM PRESSURE	vs	CAVITATION INDEX σ_1	FIGURE 5.15
UPSTREAM PRESSURE	vs	CAVITATION INDEX σ_2	FIGURE 5.16

the data being given in Tables 5.5 and 5.6.

From the graphs of pressure drop, pipe flow velocity and Reynolds Number (Figures 5.12 to 5.14), there appears to be a trend for incipient cavitation to occur at increased horizontal axis values as the upstream pressure is increased (the gr[illegible]s having positive slopes). It is also observed that as the orifice increases in size, the required pressure drop decreases for a constant upstream

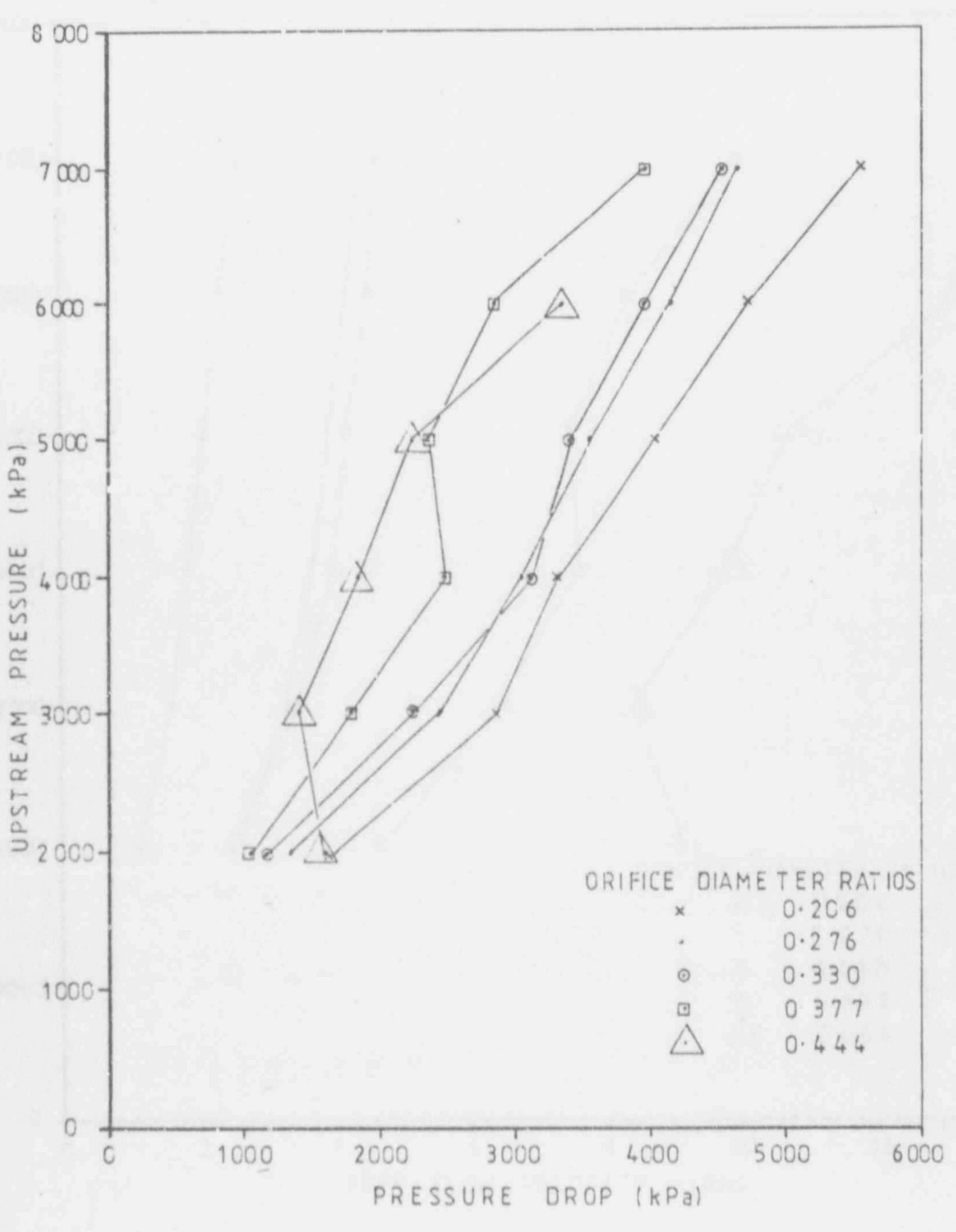

FIGURE 5.12 UPSTREAM PRESSURE vs PRESSURE DROP FOR INCIPIENT CAVITATION CONDITIONS - EAST DRIEFONTEIN GOLD MINE

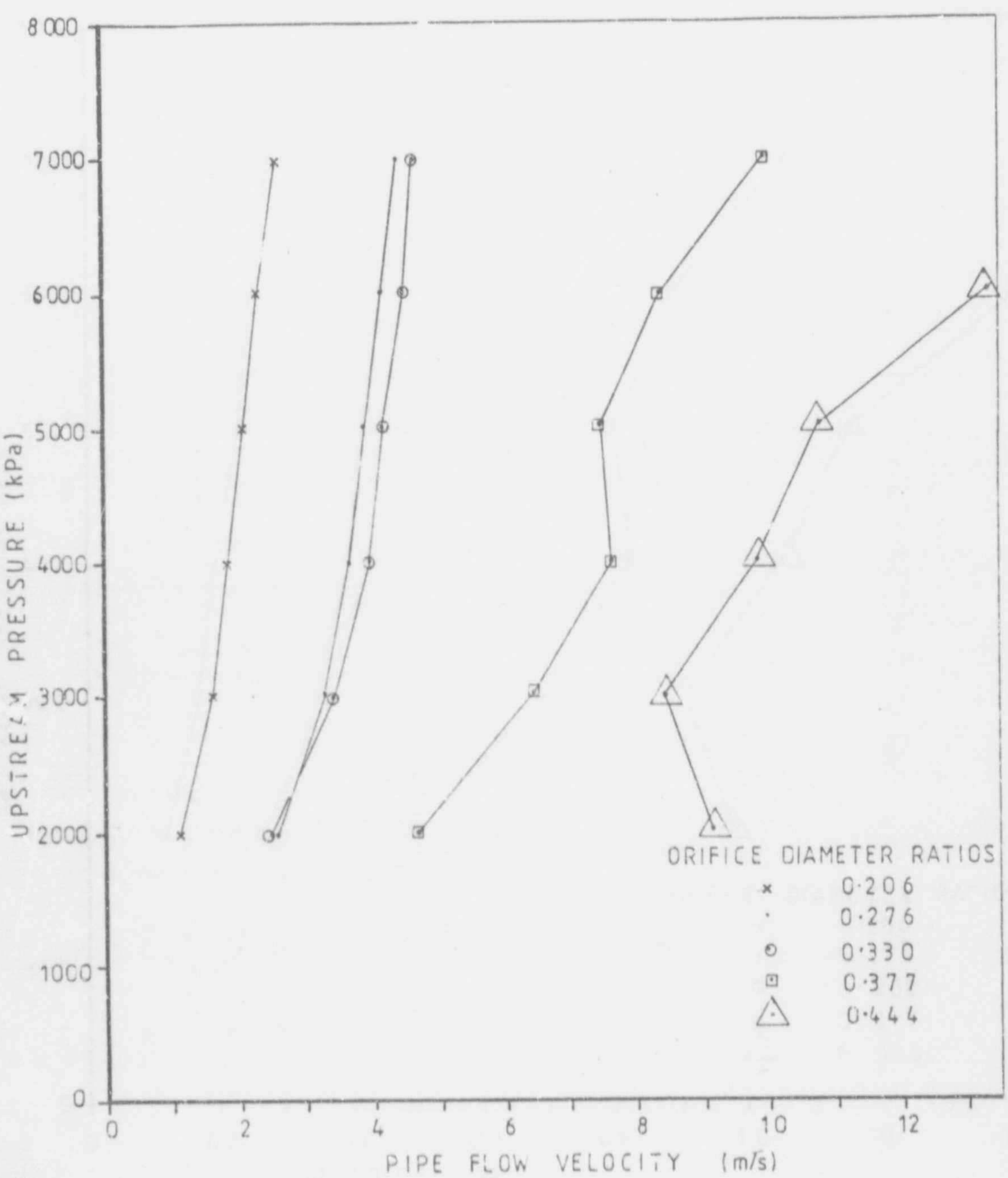

FIGURE 5.13 UPSTREAM PRESSURE vs PIPE FLOW VELOCITY FOR INCIPIENT CAVITATION CONDITIONS - EAST DRIEFONTEIN GOLD MINE

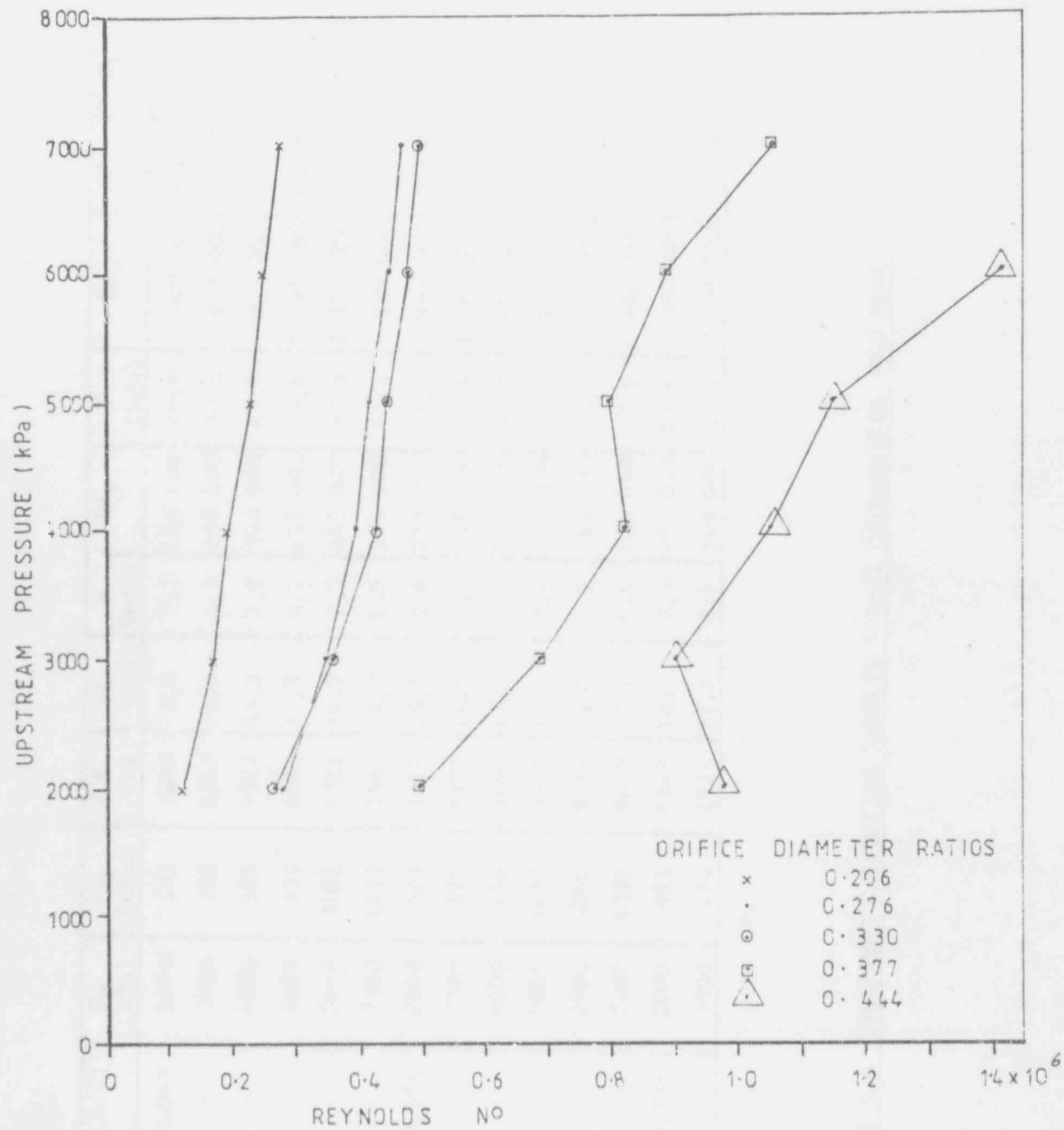

FIGURE 5.14 UPSTREAM PRESSURE vs REYNOLDS NUMBER FOR INCIPIENT CAVITATION CONDITIONS - EAST DRIEFONTEIN GOLD MINE

D (mm)	d (mm)	d/D	$(d/D)^2$	P_U (kPa)	P_D (kPa)	ΔP (kPa)	Q (l/s)	V (m/s)	Re_v	U (m/s)	Re_u	σ_i	σ_ℓ
97,2	20	0,206	0,042	2000	391	1609	8,0	1,1	116 000	26,0	566 000	0,241	0,32
-	-	-	-	3000	150	2850	11,9	1,6	169 000	37,8	823 000	0,052	0,058
-	-	-	-	4000	683	3317	13,3	1,8	190 000	42,5	925 000	0,205	0,21
-	-	-	-	5000	935	4065	15,3	2,1	222 000	49,6	1 079 000	0,229	0,21
-	-	-	-	6000	1289	4711	16,9	2,3	243 000	54,3	1 182 000	0,273	0,244
-	-	-	-	7000	1433	5567	19,0	2,6	275 000	61,4	1 336 000	0,257	0,212
97,2	26,8	0,276	0,076	2000	623	1377	19,3	2,6	275 000	34,2	997 000	0,45	0,092
-	-	-	-	3000	57[illegible]	2429	24,6	3,3	349 000	43,4	1 266 000	0,234	0,052
-	-	-	-	4000	950	3050	27,2	3,7	391 000	48,7	1 420 000	0,31	0,069
-	-	-	-	5000	1452	3542	29,0	3,9	412 000	51,3	1 496 000	0,41	0,096
-	-	-	-	6000	1866	4134	31,0	4,2	444 000	55,2	1 610 000	0,45	0,106
-	-	-	-	7000	2332	4668	32,7	4,4	465 000	57,9	1 688 000	0,499	0,121
97,2	32,1	0,33	0,109	2000	853	1147	18,6	2,5	264 000	22,9	800 000	0,741	0,136
-	-	-	-	3000	774	2226	25,3	3,4	360 000	31,2	1 090 000	0,346	0,067

TABLE 5.5 INCIPIENT CAVITATION RESULTS - EAST DRIEFONTEIN GOLD MINE

D (mm)	d (mm)	d/D	$(d/D)^2$	P_U (kPa)	P_D (kPa)	ΔP (kPa)	Q (l/s)	V (m/s)	Re_v	U (m/s)	Re_u	σ_i	σ_ℓ
97,2	32,1	0,33	0,109	4000	891	3109	29,5	4,0	423 000	36,7	1 280 000	0,286	0,056
–	–	–	–	5000	1509	3491	31,1	4,2	444 000	38,5	1 340 000	0,431	0,086
–	–	–	–	6000	2025	3975	33,1	4,5	476 000	41,3	1 440 000	0,509	0,100
–	–	–	–	7000	2445	4555	35,2	4,7	497 000	43,1	1 510 000	0,536	0,111
97,2	36,7	0,377	0,142	2000	987	1013	35,2	4,7	497 000	33,0	1 320 000	0,971	0,045
–	–	–	–	3000	1208	1792	48,2	6,5	687 000	45,6	1 820 000	0,672	0,029
–	–	–	–	4000	1538	2462	57,4	7,7	814 000	54,0	2 160 000	0,623	0,026
–	–	–	–	5000	2692	2308	55,4	7,5	793 000	52,6	2 100 000	1,165	0,048
–	–	–	–	6000	3140	2860	62,3	8,4	888 000	58,9	2 350 000	1,097	0,045
–	–	–	–	7000	3086	3914	74,0	10,0	1 058 000	70,1	2 800 000	0,787	0,031
97,2	43,2	0,444	0,198	2000	381	1619	68,1	9,2	973 000	46,6	2 190 000	0,232	0,0045
–	–	–	–	3000	1610	1390	62,9	8,5	899 000	43,0	2 020 000	1,156	0,022
–	–	–	–	4000	2138	1862	73,2	9,9	1 047 000	50,1	2 360 000	1,147	0,022
–	–	–	–	5000	2795	2205	79,8	10,8	1 142 000	54,7	2 570 000	1,266	0,024
–	–	–	–	6000	2649	3351	99,1	13,4	1 417 000	67,8	3 190 000	0,789	0,015

TABLE 5.6 INCIPIENT CAVITATION RESULTS – EAST DRIEFONTEIN GOLD MINE

pressure; and from an examination of the Reynolds Number, a higher level of turbulence is required as the orifice size increases, Figure 5.14. (The occurrence of turbulence is considered to be a function of Reynolds Number).

When considering the cavitation indices σ_1 and σ_2 (Figures 5.15 and 5.16), there is seen to be no clear trend for σ_1 or σ_2 to either increase or decrease as the upstream pressure is increased, for the same orifice size. For increasing orifice size, the σ_1 index appears to increase in value for the same upstream pressure, and the σ_2 index appears to decrease in value for the same upstream pressure; the lack of clarity shown in Figures 5.15 and 5.16 possibly results from a combination of the method used to determine the incipient cavitation point, and from the technique used to measure cavitation vibration. Furthermore, on examination of the data in Table 5.4 (Figures 5.17 & 5.18), the 0.206 diameter ratio orifice shows the predicted incipient cavitation pressures to be greater than the experimental calculated results. For the other orifice ratios this is gradually reversed, with the predicted values for the 0.444 diameter ratio orifice being less than for the experimental results. This possibly highlights a danger of using a prediction equation outside its range of use. Also, it is interesting to note that the aural incipient cavitation results yielded values broadly similar to the predicted and calculated experimental results, indicating that should no other method be available, the aural method could still be used.

In the work of Ball J.W. et al (1975), reference is made to pressure (upstream) scale effects; referring specifically to the incipient cavitation condition, it is reported that no pressure scale effect is present, i.e. for the same pipe diameter and orifice ratio, the cavitation index σ_1 remains constant for all upstream pressures. Examining the experimental results presented in Figures 5.15, 5.17, & 5.18, the reported lack of pressure scale effect cannot be validated or invalidated, since, as mentioned above, no clear trends are exhibited and there is a reversal of order of the predicted and experimental values.

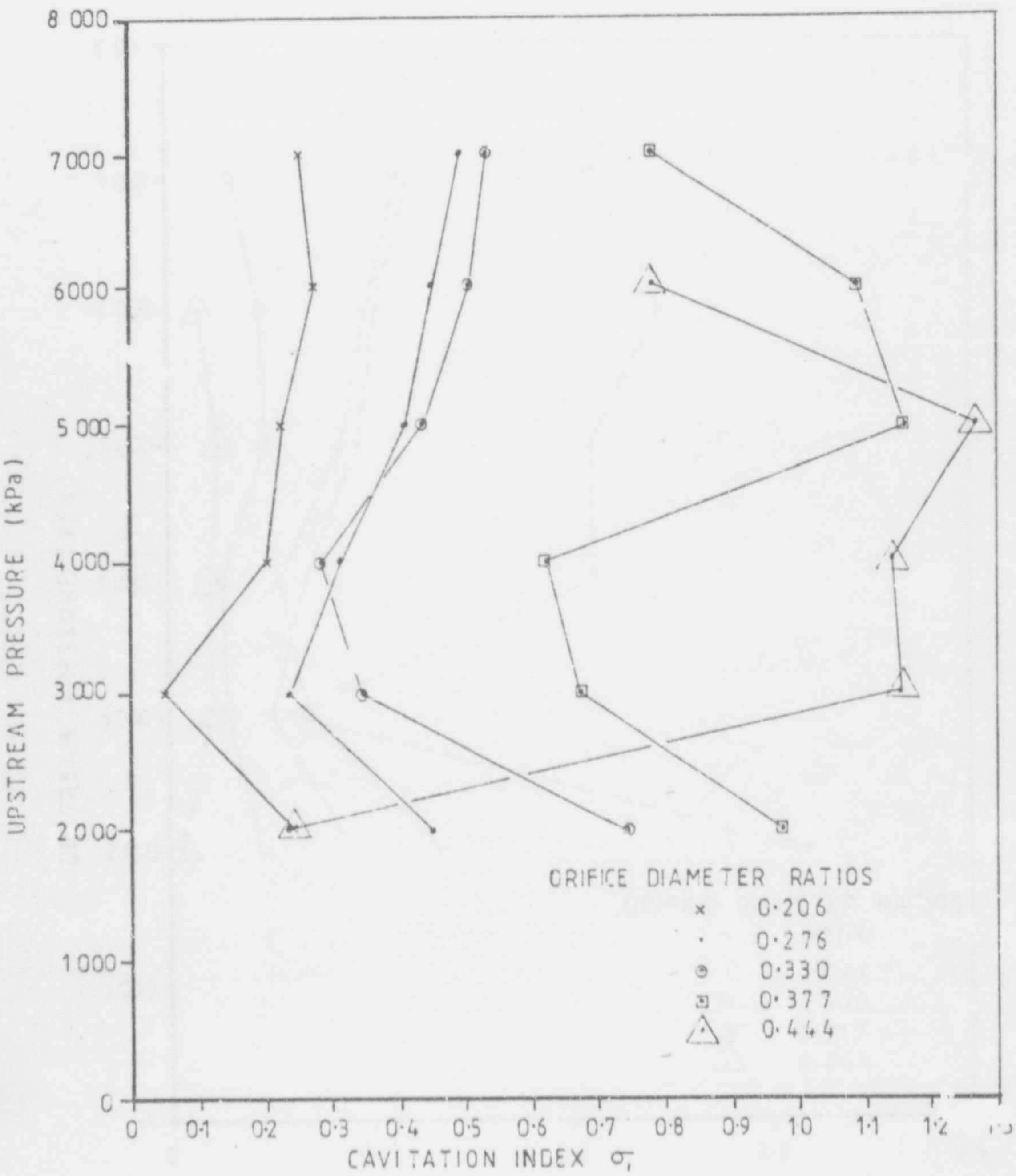

FIGURE 5.15 UPSTREAM PRESSURE vs CAVITATION INDEX σ_1 FOR INCIPIENT CAVITATION CONDITIONS - EAST DRIEFONTEIN GOLD MINE

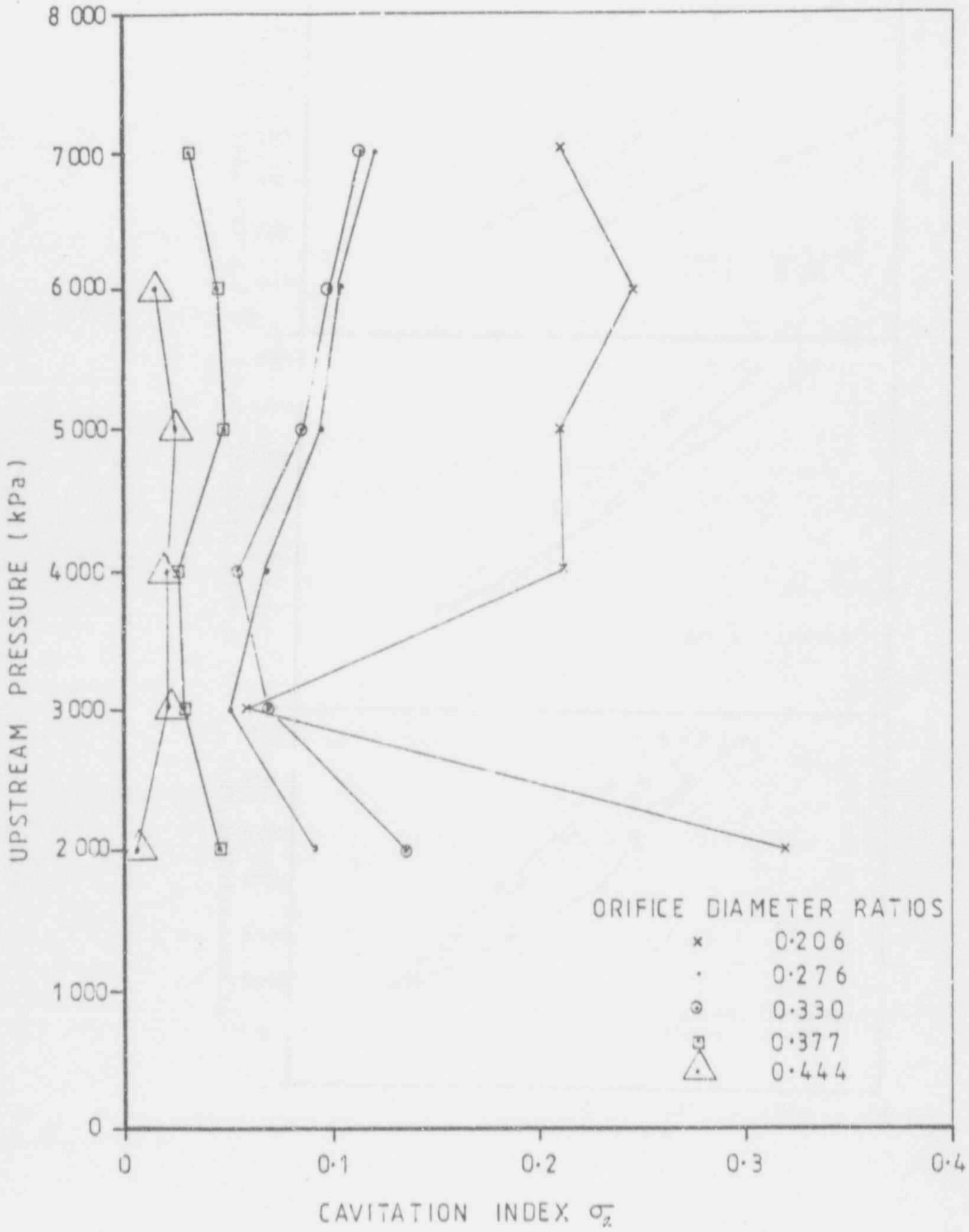

FIGURE 5.16 UPSTREAM PRESSURE vs CAVITATION INDEX σ_2 FOR INCIPIENT CAVITATION CONDITIONS - EAST DRIEFONTEIN GOLD MINE

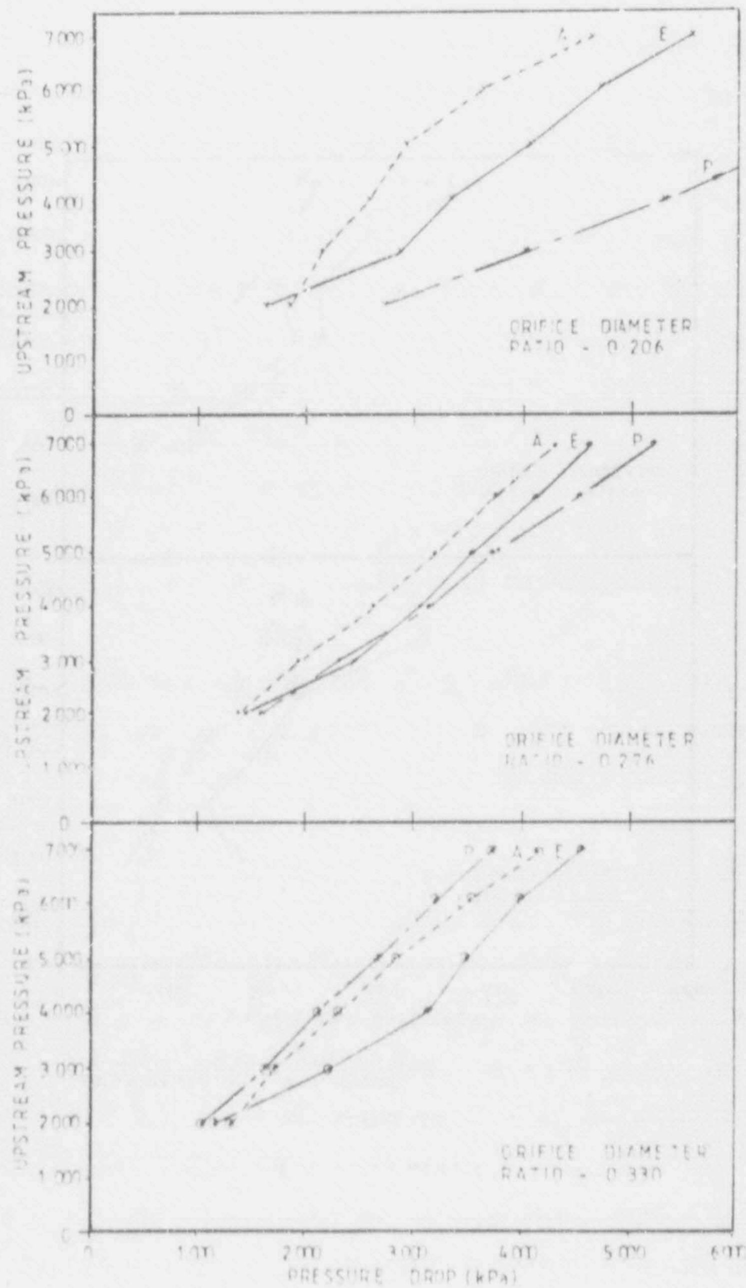

FIGURE 5.17 AURAL, PREDICTED AND EXPERIMENTAL INCIPIENT CAVITATION POINTS

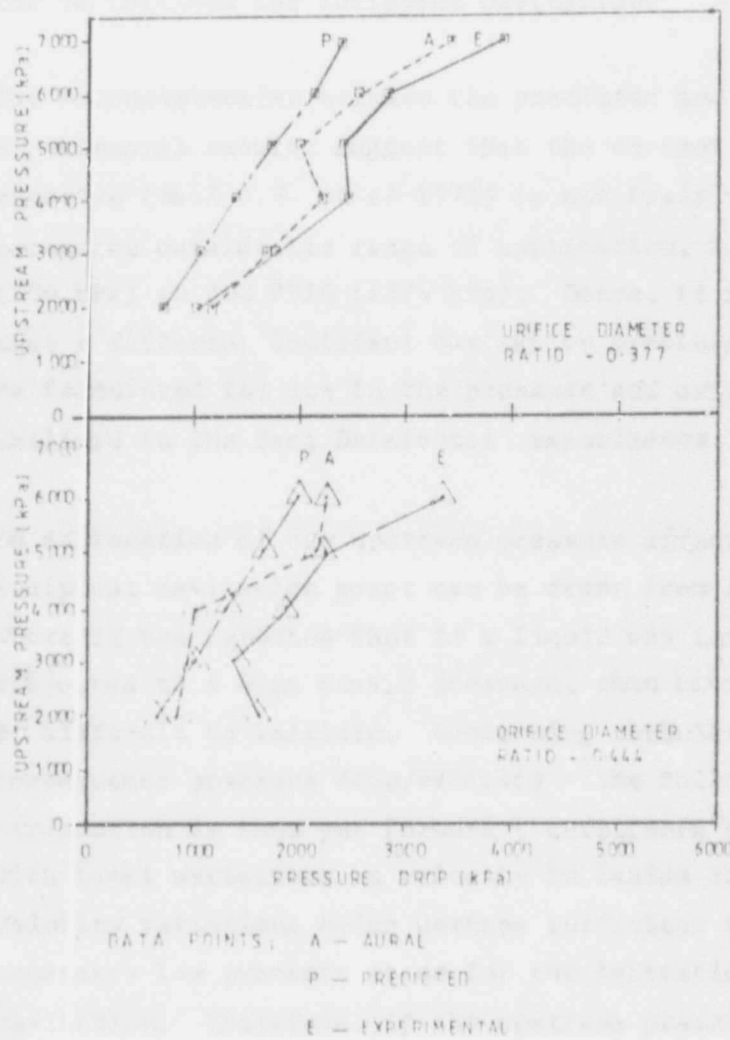

FIGURE 5.18 AURAL, PREDICTED AND EXPERIMENTAL INCIPIENT CAVITATION POINTS

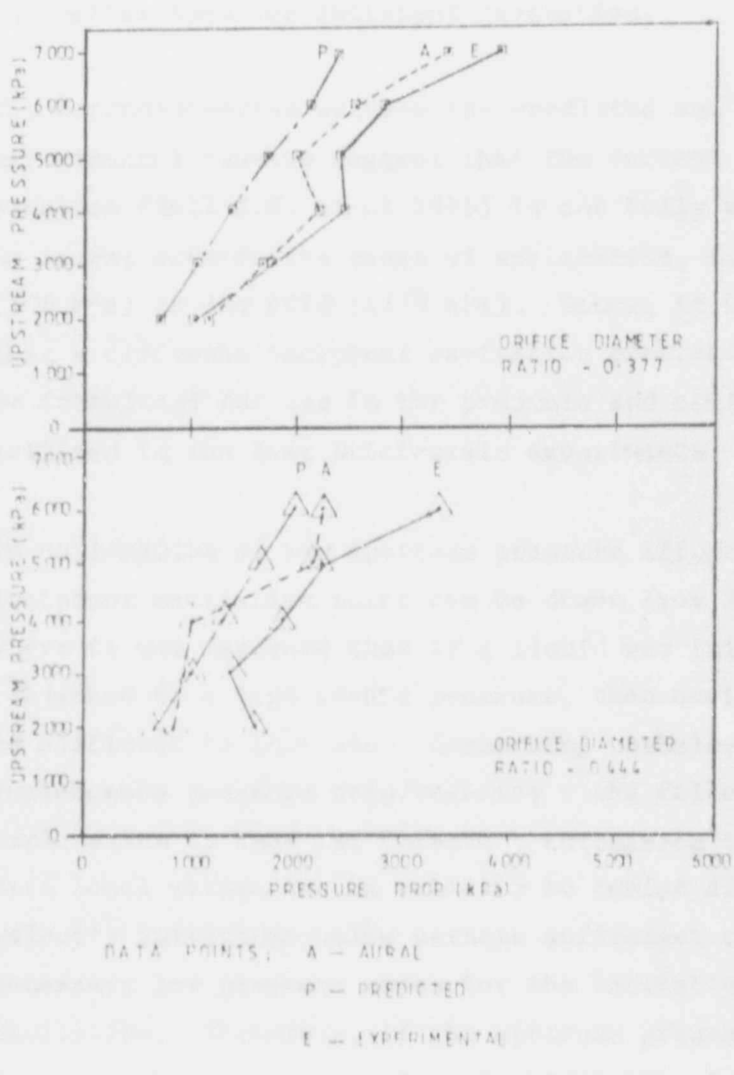

FIGURE 5.18 AURAL, PREDICTED AND EXPERIMENTAL INCIPIENT CAVITATION POINTS

The above tends to indicate that the phenomenon of cavitation - and specifically the definition of the incipient cavitation point - is not as precise in its nature as may at first appear. Perhaps this is also an indication that some of the factors discussed in Chapter 2 play an important role in cavitation prediction, along with the definitions for incipient cavitation.

The inconsistencies between the predicted and calculated experimental results suggest that the current prediction equation (Ball J.W. et al 1975) is not fully valid for pressures outside its range of application, i.e. 30 PSIG (206 kPa) to 200 PSIG (1379 kPa). Hence, it is proposed that a different incipient cavitation prediction equation be formulated for use in the pressure and orifice range utilised in the East Driefontein experiments.

An explanation of how upstream pressure affects the incipient cavitation point can be drawn from Section 2.2.2, where it was reported that if a liquid was initially subjected to a high static pressure, then cavitation would be difficult to initiate. Concerning turbulence - and in consequence pressure drop/velocity - the following explanation is thus put forward : turbulence is associated with local variations in velocity in random directions, the velocity variations being perhaps sufficient to create the necessary low pressure zones for the initiation of cavitation. Therefore, if the upstream pressure acts to suppress the occurrence of cavitation, then a higher level of turbulence will be required to overcome the suppression, and so initiate cavitation (the turbulence is possibly set up by the pump or the piping system).

To explain the change in turbulence level for the various orifice sizes used, it can be seen that the velocity or Reynolds Number required for incipient cavitation tends to increase as the orifice size increases, or conversely, the pressure drop decreases. Thus, the higher the flow velocity, the higher the turbulence as the orifice size increases, while so does the balance between suppression due to upstream pressure and turbulence shift; this latter is reflected as a decrease in pressure drop for an increase in orifice size.

To examine the experimental incipient cavitation results in terms of downsteam pressure the following graphs were drawn :

DOWNSTREAM PRESSURE	vs	CAVITATION INDEX σ_1	FIGURE 5.19
DOWNSTREAM PRESSURE	vs	CAVITATION INDEX σ_2	FIGURE 5.20
DOWNSTREAM PRESSURE	vs	PRESSURE DROP	FIGURE 5.21
DOWNSTREAM PRESSURE	vs	PIPE FLOW VELOCITY	FIGURE 5.22
DOWNSTREAM PRESSURE	vs	REYNOLDS NUMBER	FIGURE 5.23

The relevant data is also contained in Tables 5.5 and 5.6.

The same comments apply as for the upstream pressure case. However, the trends displayed for the downstream pressure cases are generally less distinct. This is ascribed to the method used to determine downstream pressure for the incipient cavitation points, downstream pressure being calculated from the incipient pressure drop and the controlled upstream pressure.

For the experimental flow/pressure drop measurements, all data are plotted in Figure 5.24, along with predicted data. The graph indicates that the experimental values are generally consistent with the theoretical values (the exception being for the 0,206 diameter ratio orifice). This is also in line with the calculated root mean square deviations for the fitted equations (Table 4.1). The difference of the 0,206 diameter ratio orifice is thought to be due to one of three reasons, or possibly combinations of them. For example, there could have been a systematic error in measurement. However, the error would then be

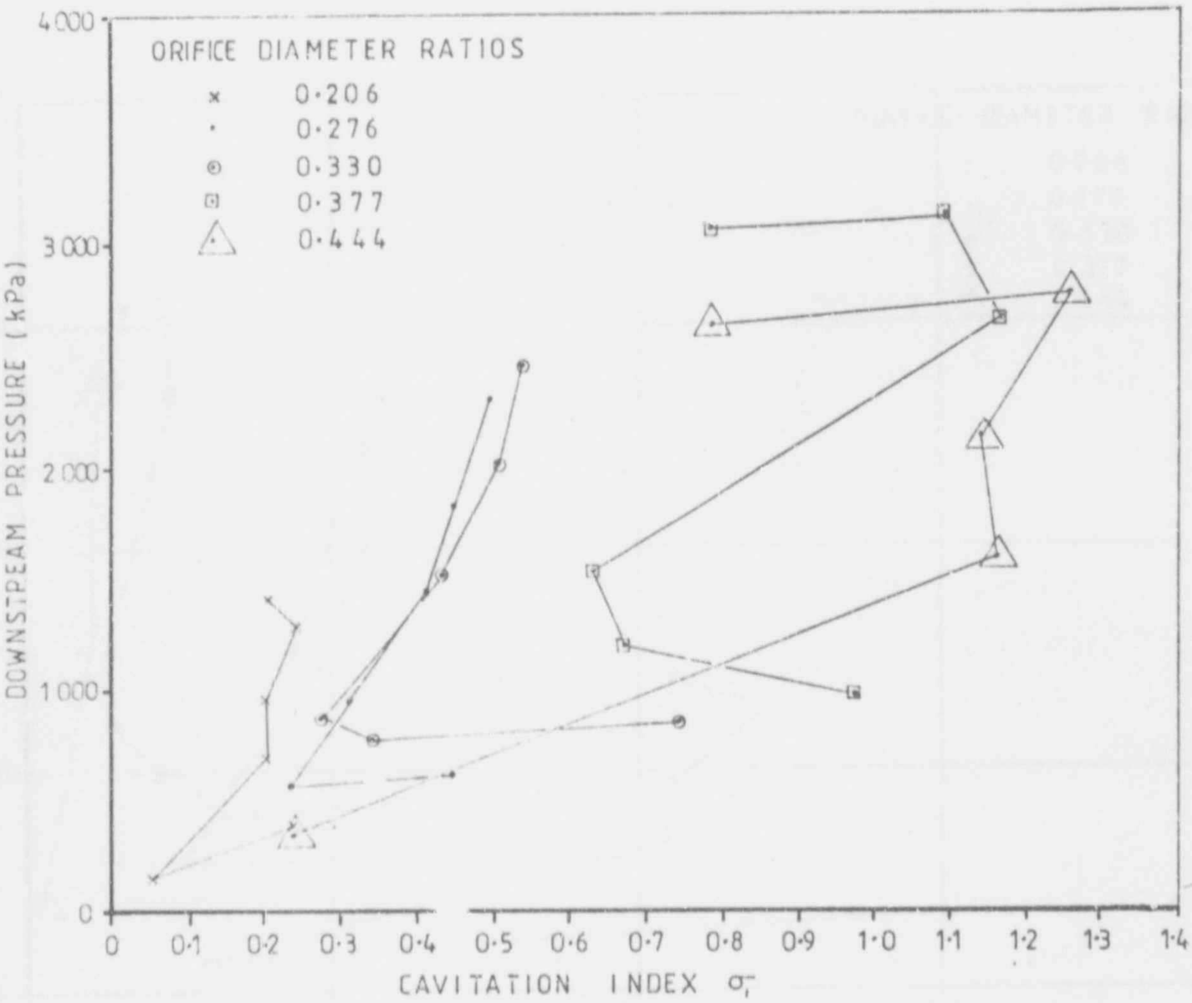

FIGURE 5.19 DOWNSTREAM PRESSURE vs CAVITATION INDEX σ_1 FOR INCIPIENT CAVITATION CONDITIONS - EAST DRIEFONTEIN GOLD MINE

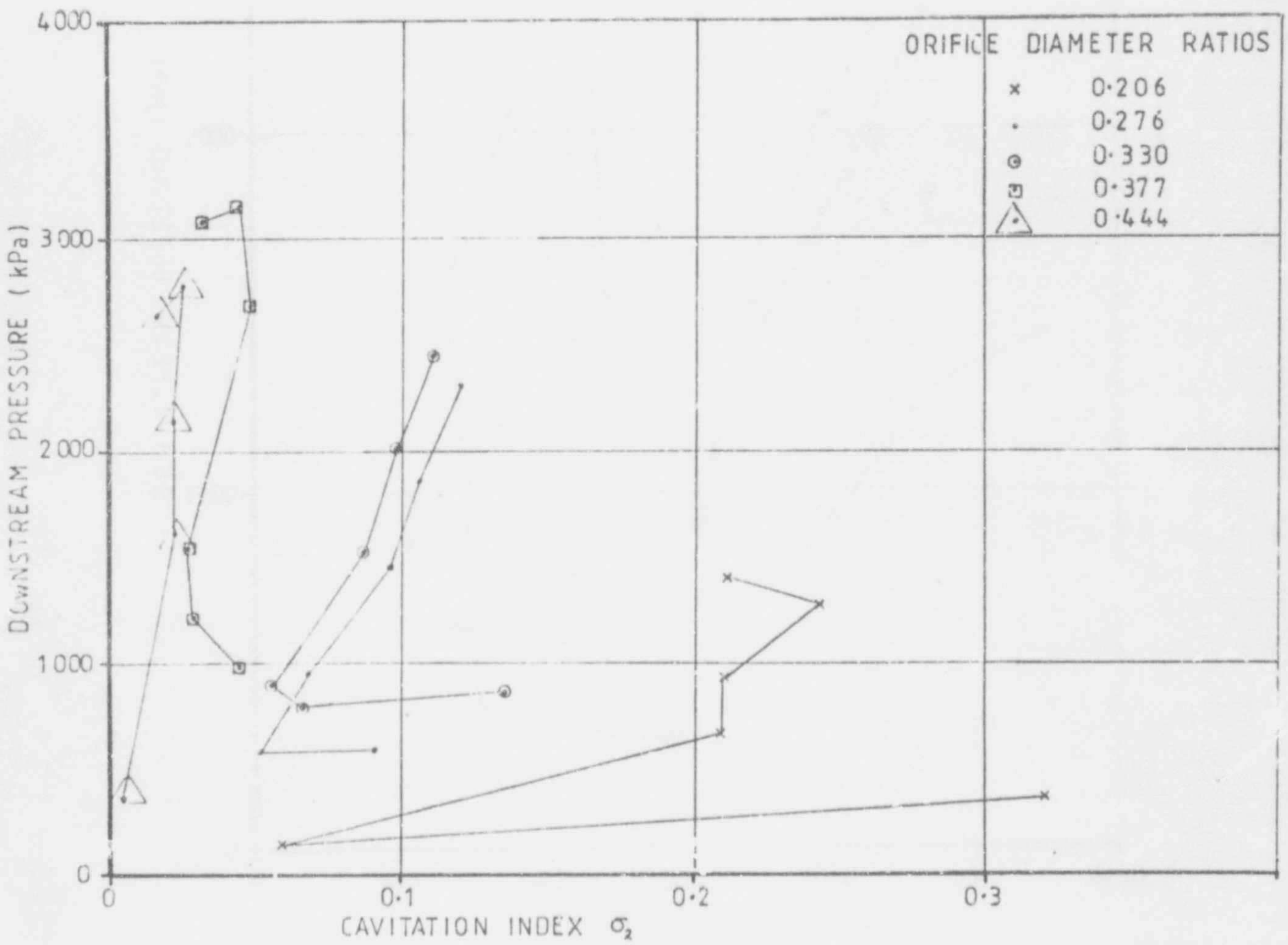

FIGURE 5.20 DOWNSTREAM PRESSURE vs CAVITATION INDEX σ_2 FOR INCIPIENT CAVITATION CONDITIONS - EAST DRIEFONTEIN GOLD MINE

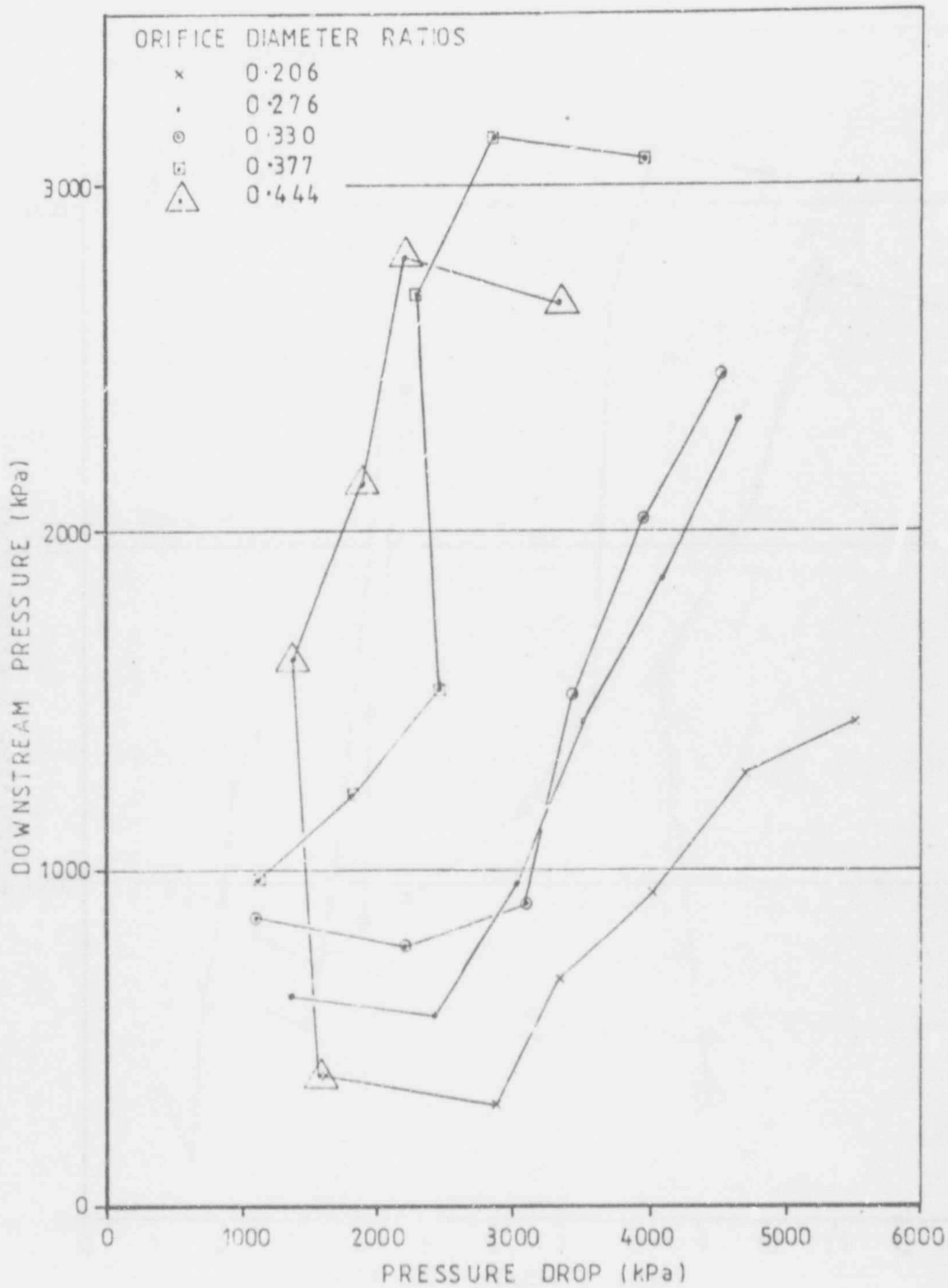

FIGURE 5.21 DOWNSTREAM PRESSURE vs PRESSURE DROP FOR INCIPIENT CAVITATION CONDITIONS - EAST DRIEFONTEIN GOLD MINE

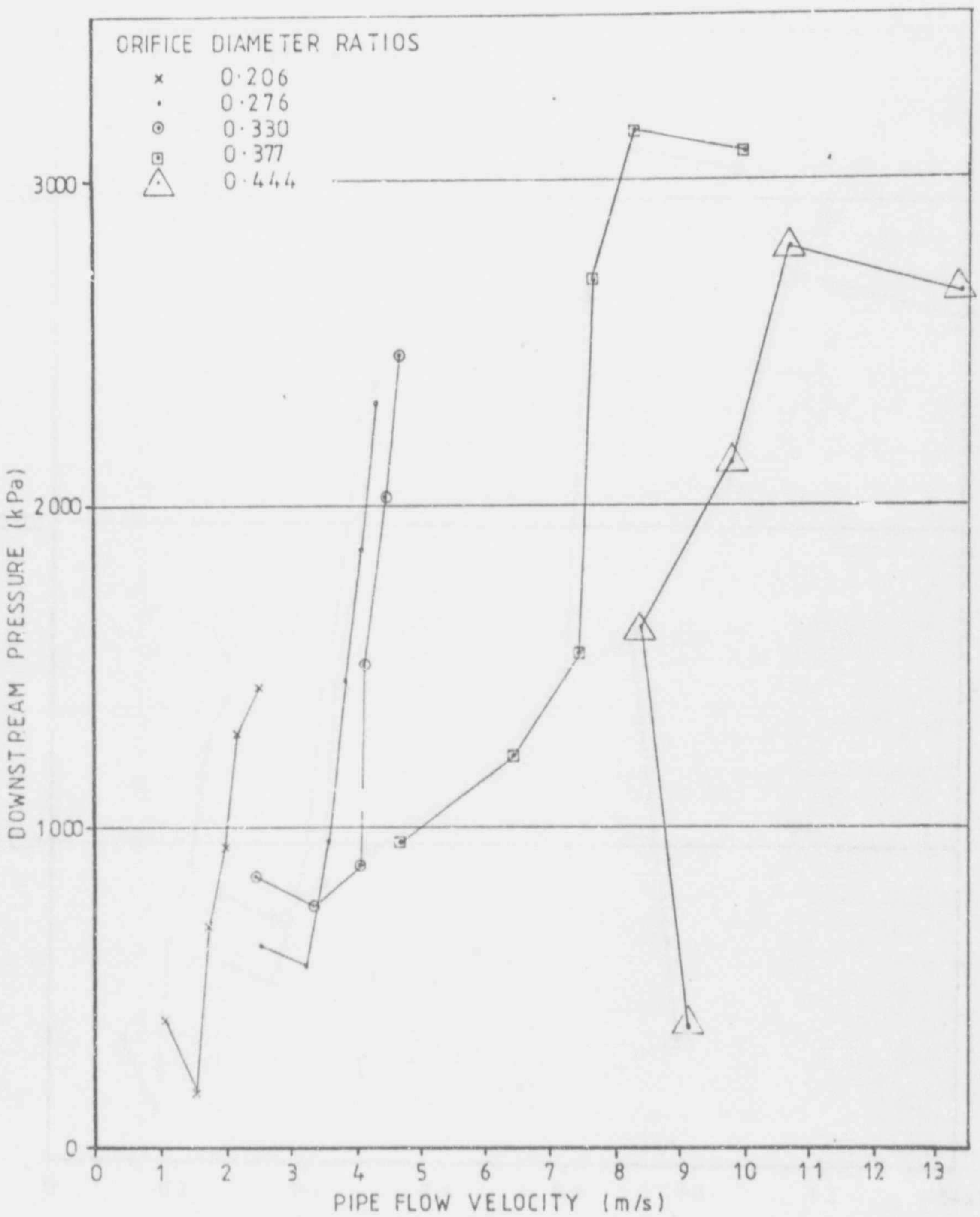

FIGURE 5.22 DOWNSTREAM PRESSURE vs PIPE FLOW VELOCITY FOR INCIPIENT CAVITATION CONDITIONS - EAST DRIEFONTEIN GOLD MINE

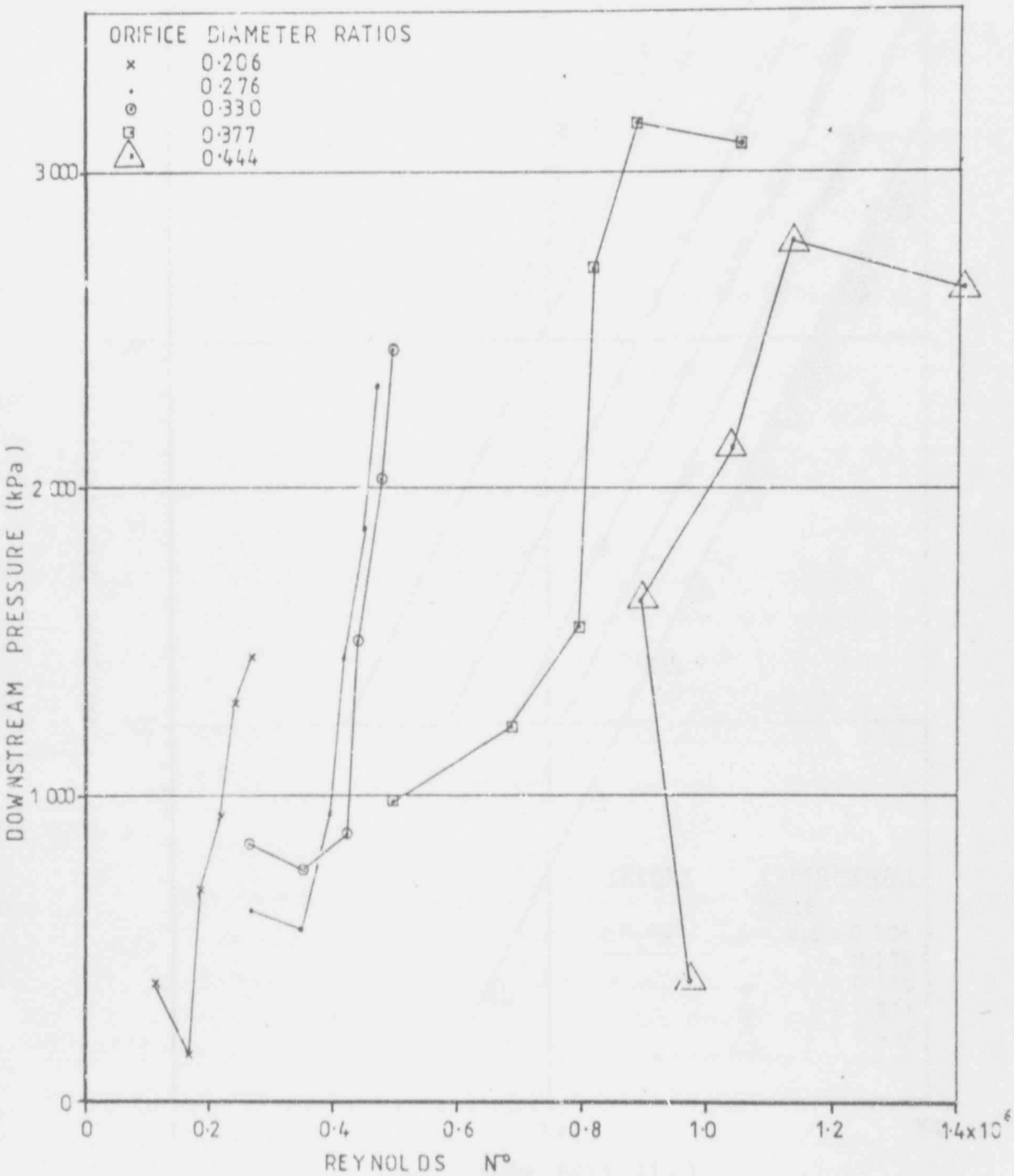

FIGURE 5.23 DOWNSTREAM PRESSURE vs REYNOLDS NUMBER FOR INCIPIENT CAVITATION CONDITIONS - EAST DRIEFONTEIN GOLD MINE

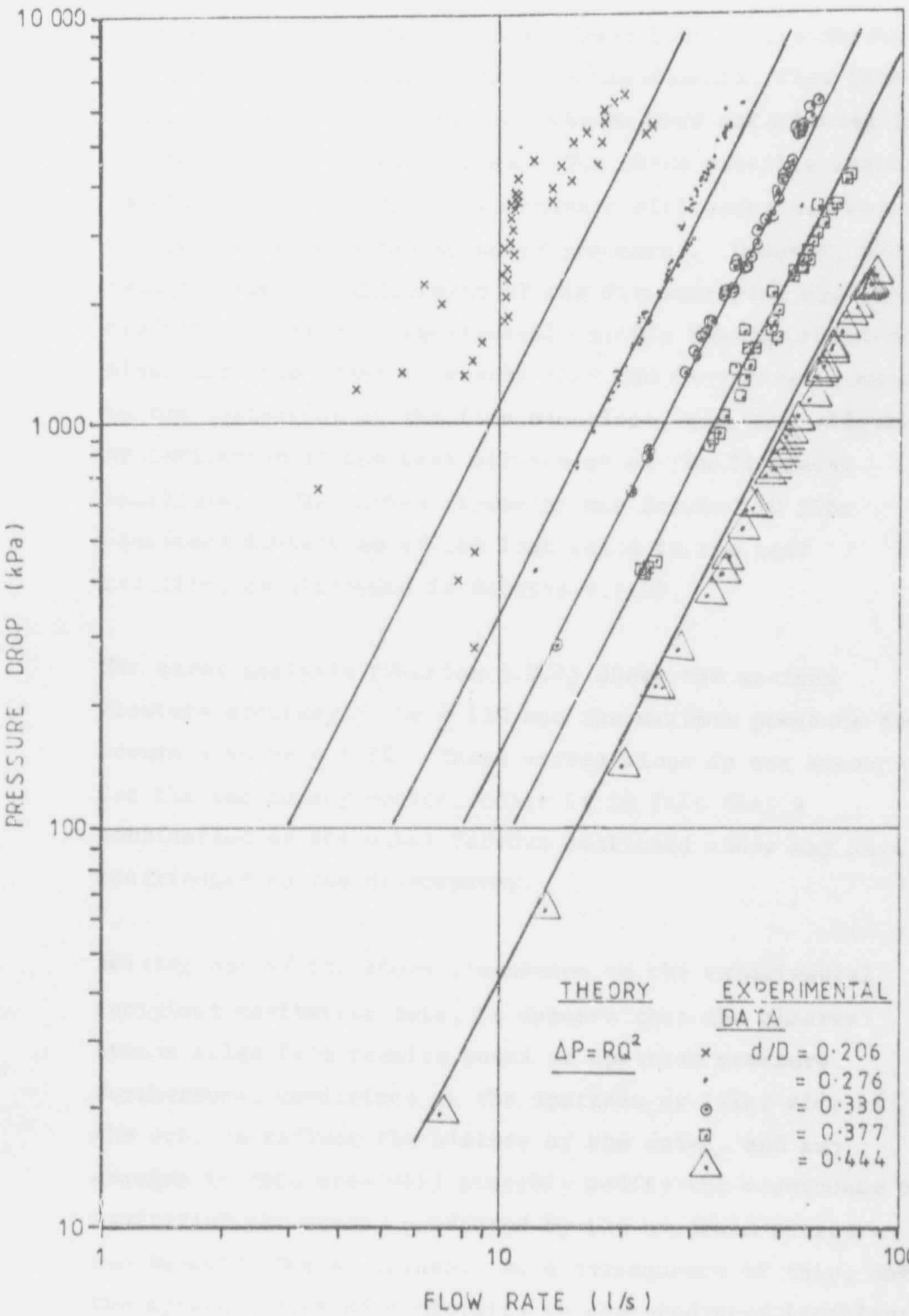

FIGURE 5.24 ORIFICE FLOW vs PRESSURE DROP - EAST DRIEFONTEIN GOLD MINE

similar in each case. There may have been an inaccuracy in the methods used to determine the experimental flow rates, bearing in mind that certain problems were experienced in the measurement of flow rates. The third possible reason is that cavitating flow (two phase : air/vapour and water) causes a change in the measured pressures. However, the results from the University of the Witwatersrand show that cavitation does not significantly modify flow measurement. Also, care was taken to ensure that the flow results used in the derivation of the flow equations, were not affected by cavitation at the test orifice or at the flowmeter locations. (The vortex flowmeter was located 30 pipe diameters downstream of the last valve in the test facility, as discussed in Section 4.2.2).

The error analysis (Section 5.2.2) shows the maximum flowrate accuracy to be $\pm$ 11% and the maximum pressure drop accuracy to be $\pm$ 2,7%. These errors alone do not account for the inaccuracy quoted, hence it is felt that a combination of the other factors mentioned above may have contributed to the discrepancy.

Arising out of the above discussion on the experimental incipient cavitation data, it appears that the clearest trends arise from results based on upstream pressure. Furthermore, conditions at the upstream or inlet side of the orifice reflect the history of the water, and any changes in this area will possibly modify the occurrence of cavitation phenomena, predicted by the upstream pressure and Reynolds Number values. As a consequence of this, and the apparent lack of conformity to the predicted incipient cavitation data, an empirical equation (as suggested earlier) will be formulated to predict incipient cavitation in the following section, this will be based on orifice ratio, upstream pressure and pressure drop. Also, in an attempt to explain how upstream pressure affects bubble growth, the Poritsky analysis developed in Section 2.1.3 will also be applied to the inception results.

5.3 ANALYSIS OF RESULTS

One of the observations arising from the figures presented in Section 5.2 was that as upstream pressure increased, the pressure drop required for incipient cavitation also increased. The following analysis offers an explanation for this observation. The analysis is based on the Poritsky critical radius requirement (Section 2.1.3) and the characteristic equation of state for a perfect gas. Furthermore, an estimate is made of the number of bubbles produced at cavitation inception, and an indication is given as to how these bubbles could physically fit into the orifice flow.

5.3.1 PORITSKY CRITICAL RADIUS

The Poritsky critical radius equation is

$$R_{CR} = \left(\frac{9 R_* T m}{8 \pi S} \right)^{0.5} \qquad 5.27$$

and the characteristic equation of state for a perfect gas is

$$\frac{P V}{T} = R \qquad 5.28$$

It should be noted that in using the above equations, certain assumptions have been made, which are:

i) a free bubble remains spherical at all times.

ii) the gas/vapour contained in the bubble behaves as a perfect gas.

iii) no temperature changes occur.

iv) no evaporation or condensation occurs at the bubble wall.

With the water initially at relatively low pressure (atmospheric pressure), it is assumed that all bubbles have a radius of 0,1 mm. As the upstream pressure changes the bubble size also changes, values being given in Table 5.7 below.

PRESSURE (kPa)	RADIUS (m)	VOLUME (m^3)
2000	$3{,}6 \times 10^{-5}$	2×10^{-13}
3000	$3{,}2 \times 10^{-5}$	$1{,}4 \times 10^{-13}$
4000	$2{,}9 \times 10^{-5}$	1×10^{-13}
5000	$2{,}7 \times 10^{-5}$	$8{,}2 \times 10^{-14}$
6000	$2{,}5 \times 10^{-5}$	$6{,}9 \times 10^{-14}$
7000	$2{,}4 \times 10^{-5}$	$5{,}9 \times 10^{-14}$

TABLE 5.7 BUBBLE DIMENSIONS FOR VARIOUS UPSTREAM PRESSURES

Furthermore, it is assumed that the perfect gas contained in the bubbles has a density of 1,0 kg/m^3, thus the mass of each bubble is constant at $4{,}2 \times 10^{-12}$ kg. Using the critical radius equation given above, the critical radius is found to be $1{,}7 \times 10^{-3}$m, giving a bubble volume of 2,1 x 10^{-8}m. Comparing these values to those in Table 5.7, it is observed that the change in bubble radius required before the critical radius is attained increases with an increase in upstream pressure, thus indicating that an increase in energy is required for cavitation inception, as the upstream pressure is increased. This is a similar result to that predicted in Section 2.1.3, ie. the energy required for cavitation inception changes with bubble size and pressure. The experimental results for incipient cavitation from East Driefontein indicate that the required mean orifice flow velocity increases with upstream pressure, thereby indicating that an increase in kinetic energy is required.

From the above example of initial and critical radii, an estimate of the energy required for inception can be made. At 2000 kPa the bubble radius changes from $3,6 \times 10^{-5}$m to $1,7 \times 10^{-3}$m (a 47-fold change), and volume from $2 \times 10^{-13}m^3$ to $2,1 \times 10^{-8}m^3$ (a 105 000-fold change).
At 7000 kPa, the radius changes from $2,4 \times 10^{-5}$m to $1,7 \times 10^{-3}$m (a 71-fold change), and the volume from $5,9 \times 10^{-14}m^3$ to $2,1 \times 10^{-8}m^3$ (a 356 000-fold change).
With reference to the East Driefontein experiments, one particular orifice size, namely that for which d/D = 0,[illegible]76, and assuming the process of bubble expansion to be a non-flow process, the energy required can be calculated from the expression:

$$w = \int_1^a P\,dv \qquad 5.29$$

Assuming that $Pv = C$ 5.30

then $$w = P_1 V_1 \ln \frac{V_a}{V_1} \qquad 5.31$$

Evaluating this for the above example, the energy required per bubble (mass = $4,2 \times 10^{-12}$kg) becomes

$4,62 \times 10^{-6}$ J at 2000 kPa
$5,28 \times 10^{-6}$ J at 7000 kPa

Equating to

$1,1 \times 10^{-6}$ J/kg at 2000 kPa
$1,26 \times 10^{-6}$ J/kg at 7000 kPa

These values combine to give energy gradient of 320×10^6 J/kPa, and a linear equation, viz.

Energy per bubble kg $= 320 \times 10^{6}(\mathrm{J/kPa}) \times P(\mathrm{kPa}) + 0,46 \times 10^{6}(\mathrm{J})$

This is qualitatively consistent with the experimental results, namely that an increase in energy is required to cause cavitation inception as the upstream pressure increases.

In this analysis it is realised that there are certain inherent limitations. These are the fact that a bubble maintains a constant mass (no evaporation or condensation occurs at the bubble wall), and (perhaps more important) the fact that a bubble is assumed to be at constant temperature. Departures from both of these conditions would affect the rate of bubble growth. It should also be noted that the analysis is for one bubble size only, whereas in a real situation there would be a range of bubble sizes.

From the above, it is theoretically possible to estimate the number of bubbles produced at inception, per unit mass (unit volume). This is done by calculating the increase in kinetic energy between upstream conditions and the orifice

$$w = \frac{m(V_1^2 - V_2^2)}{2} \qquad 5.32$$

and assuming that the initial bubble sizes in the flow are the same as those given in Table 5.7, the number of bubbles per unit mass can be calculated from

$$\text{No of bubbles} = \frac{\text{Energy available at orifice}}{\text{Energy for bubble formation}} \qquad 5.33$$

Furthermore, the number of bubbles per kg of water can also be calculated at the orifice exit using the water density (1000 kg/m^3) and critical bubble volume.

$$\text{No. of Bubbles} = \frac{\text{Volume of 1 kg water}}{\text{Critical bubble volume}} \qquad 5.34$$